An effective hybrid organic/inorganic inhibitor for alkaline aluminum-air fuel cells

Yujuan Nie[a,b,1], Jianxin Gao[b,1], Erdong Wang[b,*], Luhua Jiang[b], Liang An[c], Xuyun Wang[a,**]

[a] College of Chemical Engineering, Qingdao University of Science and Technology, Qingdao 266042, China
[b] Division of Fuel Cell & Battery, Dalian National Laboratory for Clean Energy, Dalian Institute of Chemical Physics, Chinese Academy of Sciences, Dalian 116023, China
[c] Department of Mechanical Engineering, The Hong Kong Polytechnic University, Hung Hom, Kowloon, Hong Kong Special Administrative Region, China

ARTICLE INFO

ABSTRACT

An issue associated with aluminum-based batteries is the drastic parasitic corrosion of aluminum anode, which significantly restricts the utilization of aluminum. An effective approach is to add inhibitors in electrolytes to reduce the anode corrosion rate. In this work, Na_2SnO_3 and casein are proposed to act as a hybrid inhibitor in alkaline aluminum-air fuel cell. It is demonstrated that $0.05\,M\,Na_2SnO_3$ and $0.6\,g\,L^{-1}$ casein offers the strongest corrosion protection, reducing the corrosion rate by approximately one order of magnitude. The corrosion inhibition is mainly attributed to the inhibition of cathodic reaction process. In addition, the analysis on the morphology and composition of the aluminum surface suggests that casein can greatly promote the deposition of tin to form a uniform and stable layer on the aluminum surface, due to the strong adsorption of polar functional groups in casein. Furthermore, the use of the hybrid inhibitor in aluminum-air fuel cell contributes to an increase of discharge capacity by 89.3%.

© 2017 Elsevier Ltd. All rights reserved.

1. Introduction

Metal-air fuel cells (MAFCs) are electrochemical energy conversion devices that directly convert chemical energy stored in metal (e.g. Mg, Al, or Zn) into electrical energy. MAFCs have drawn considerable attention in recent years because they offer many unique advantages, such as environmental friendliness [1]. Among MAFCs, aluminum-air fuel cell is regarded as an attractive candidate due to its high theoretical energy density (8100 Wh kg^{-1}), mechanical rechargeability and recyclable product (i.e., Al(OH)$_3$). Moreover, aluminum is the most geologically abundant metal with a very negative thermodynamic electrode potential of $-2.31\,V$ vs. SHE in alkaline media [2–5]. These superiorities of aluminum-air fuel cell make it become a promising energy source for electric vehicles, military equipment, and communication station, etc. However, the commercialization of aluminum-air fuel cell is still hampered by several technical challenges. Among them, the anode corrosion has been identified as the most challenging issue [3,4]. It is believed that an insoluble oxide film appears

spontaneously on the aluminum surface in neutral electrolytes, obstructing the active dissolution of aluminum anode [6,7]. However the surface film can be removed in strong alkaline solution, and the anode self-corrosion accompanied with hydrogen evolution gives rise to unacceptably high coulombic loss on discharge [8–10].

Numerous researchers have paid much attention to solving the anode corrosion problem, and two approaches have been mainly proposed [4,9,11–13]. On one hand, aluminum alloys are prepared to restrain corrosion by doping Ga, In, Mg, Sn and etc. in high-purity-grade aluminum, and thus negatively shift the potential of aluminum corrosion [2,11,14,15]. However, the inhibition effect of alloys is not quite well. On the other hand, the addition of inhibitors into the electrolyte solution can retard the parasitic hydrogen evolution corrosion without sacrificing the activity of aluminum anode [2], and inhibitors can act as activators of anodic dissolution [16]. For these reasons, aluminum alloys as well as inhibitors are used to weaken anode corrosion in this study.

In the past few decades, many studies have focused on different inhibitors, including inorganic, organic, or hybrid types. For the inorganic inhibitors, zinc oxide and sodium stannate are proved to be very effective to mitigate the corrosion of aluminum in alkaline solution. It is achieved by forming a loose layer composed of zinc or tin that raises the hydrogen overpotential on the surface of aluminum anodes [3,14,17–19]. Afterwards, some organics are

---

used as inhibitors, such as polyaniline [20], polypyrrole [21,22], hydroxytryptamine [23] and dimethyl amine epoxypropane [24]. Nevertheless, the inhibition effect of organic additives in alkaline solution is not very remarkable. Thus, hybrid additives which combine the effect of inorganic and organic additives begin to attract more and more attention. The corrosion behavior of pure aluminum in 4 M NaOH which contains ZnO and cetyl trimethyl ammonium bromide (CTAB) shows rather low hydrogen evolution rate, due to the formation of a protective and uniform zinc layer [3]. And also, the use of hybrid organic/inorganic inhibitor based on poly ethylene glycol di-acid and zinc oxide is proved to be significantly effective on inhibiting self–corrosion of aluminum anode [25].

Recently, due to their nontoxicity, biodegradability and low cost, amino acids have been considered as a component of hybrid inhibitors. The combination of L-cysteine and cerium nitrate can effectively retards the self-corrosion of AA5052 aluminum alloy in 4 M NaOH solution by forming a complex layer between the L-cysteine and cerium ions on the aluminum surface [2]. Then, the adsorption mode of L-cysteine molecules is proposed. The adsorption of L-cysteine on the aluminum surface obeys the amended Langmuir's adsorption isotherm and the inhibition mechanism is dominated by the geometric coverage effect [26]. The carbonyl and amino groups as well as other polar groups play a vital role in alleviating self-corrosion of aluminum, which can form complexes with metal ions on the surface of aluminum. In addition, glycine and alanine are also very useful to control self-corrosion of aluminum in alkaline solution [26,27].

Casein, a type of protein, is soluble in alkaline solution. The molecular structure of casein is shown in Fig. 1. Casein contains many polar functional groups such as carbonyl group, amide group and amino group. These polar groups can form a reticular adsorption on the surface of aluminum. Considering the action mechanism of amino acids in hybrid inhibitors, it is expected that casein molecules have more polar groups compared with single amino acid will produce stronger corrosion protection. The corrosion inhibition effect of casein has not been reported yet.

In this paper, we investigate the corrosion inhibition effect of the Na_2SnO_3 and casein hybrid inhibitor. The electrochemical behavior was studied via polarization curves. The surface crystalline structures and morphology of aluminum anode were characterized by X-ray diffraction spectroscopy (XRD) and scanning electron microscope (SEM), respectively. In addition, the performance of aluminum-air fuel cell was tested at a high current density of $100\,mA\,cm^{-2}$, which is rarely reported in literatures [2,11,14,19,28–30]. Furthermore, the inhibition mechanism of the hybrid inhibitor was proposed.

2. Experimental

2.1. Materials and chemicals

The electrolytes used in this study were 4 M NaOH with or without different additives. The concentration of casein varied
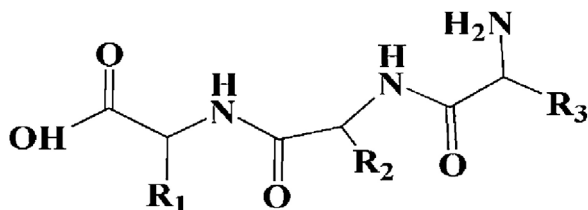
from 0.2 to $1.0\,g\,L^{-1}$ (0.2, 0.4, 0.6, 0.8 and $1.0\,g\,L^{-1}$). Na_2SnO_3 ($\geq 97.0\%$, Molbase, Tianjin) and NaOH ($\geq\geq 96.0\%$, Tianda, Tianjin) used in all experiments were of analytical grade, while casein (AoBoXing Bio-tech Co., Beijing) was a biological reagent.

Aluminum alloys used in this work were provided by Central South University, and the chemical composition of aluminum alloy is shown in Table 1. The aluminum alloy specimens were cut into pieces of $1\,cm^2$ for hydrogen evolution and electrochemical measurements, and $10\,cm^2$ for cell performance test. All the aluminum electrodes were treated by following steps. First, polished mechanically with sandpaper of silicon carbide up to 2000, then degreased with ethyl alcohol, rinsed with distilled water and dried under the condition of a steam of air.

2.2. Hydrogen evolution tests

Hydrogen is generated from the aluminum alloy in alkaline solution by the following reaction:

$$2Al + 6H_2O + 2OH^- \rightarrow 2Al(OH)_4^- + 3H_2 \tag{1}$$
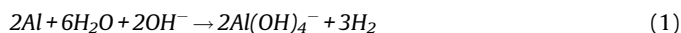
Corrosion rates were identified by measuring the volume of evolved hydrogen as the aluminum alloy samples were immersed in 50 mL solution for 1 h at $25 \pm 1\,°C$. The hydrogen collection experiment was performed in a drainage device with conical flask (50 mL), graduated cylinder (50 mL) and gas-guide tube. The hydrogen evolution rate (R) and inhibition efficiency (IE) over the immersion period were calculated according to the equation (2), (3) respectively.

$$R = \frac{V_{H_2}}{A \times t} \tag{2}$$

$$IE = \frac{R_0 - R_{inh}}{R_0} \times 100\% \tag{3}$$

where A is specimen area in cm^2, V_{H_2} is the volume of collected hydrogen gas in mL, and t is the immersion period in minute, R_0 and R_{inh} are the hydrogen evolution rates of aluminum in blank solution and in solution with different inhibitors.

2.3. Electrochemical measurements

Electrochemical measurements were performed at temperature of $25 \pm 1\,°C$ in the conventional three-electrode cell with an aluminum alloy as the working electrode (WE), a Hg/HgO electrode equipped with a Luggin-Haber capillary connecting to the solution as the reference electrode (RE) and, a platinum foil as the counter electrode (CE). The WE was a cuboid of 1 cm × 1 cm × 0.3 cm, which was sealed with epoxy resin so that only a $1\,cm^2$ of cross section was exposed. The electrochemical measurements were performed by using a Solartron 1287 Electrochemical Workstation coupled with a Solartron 1260 Impedance/Gain-Phase Analyze. The potentiodynamic polarization curves were measured from a cathodic potential of $-0.4\,V$ to an anodic potential of $+1.2\,V$ with respect to the open circuit potential (OCP) at a scan rate of 1 mV/s. The EIS experiments were carried out in the frequency range from 100 kHz to 0.01 Hz at OCP with a 5 mV amplitude. The conductivity

Fig. 1. Molecular structure of the casein (R1, R2, R3 contains different amino acid polar groups, respectively).

Table 1
Chemical compositions of aluminum alloy(wt %).

Mg	Ga	Sn	Zn	Fe	Cu	Si	Al
0.024	0.011	0.010	0.004	≤0.009	≤0.001	≤0.001	remainder

of electrolyte solutions were measured by conductivity meter (S7-Field Kit with InLab 738-ISM, Mettler Toledo).

2.4. Surface micro-morphology and composition examination

Aluminum surface evaluation was conducted after 1 h exposure under OCP in 4 M NaOH solution with different inhibitors at $25 \pm 1\,°C$. Compositional analysis of the aluminum surface layer was carried out by XRD (X'pert Pro, PANalytical B.V.) and Thermo escalab 250Xi X-ray photoelectron spectroscopy (XPS). SEM (JSM-7800F, JEOL) were used to investigate the surface morphology.

2.5. Cell tests

Aluminum-air fuel cells were constructed by an aluminum alloy anode conjugated with two air cathodes using MnO_2 as the oxygen reduction reaction catalyst (QuantumSphere, Inc.). The discharge performance of aluminum-air fuel cell was studied by means of galvanostatic discharge test at $100\,mA\,cm^{-2}$, and the cut-off voltage is 0.6 V.

3. Results and discussion

3.1. Hydrogen evolution tests

The hydrogen evolution rates of aluminum alloy in 4 M NaOH solution with different inhibitors are shown in Table 2.

It suggests that the hydrogen evolution rate of aluminum alloy in 4 M NaOH is markedly reduced with the addition of Na_2SnO_3. When the concentration of Na_2SnO_3 is 0.07 M, the hydrogen evolution rate is lowest. It has been interpreted that tin plating onto cathodic sites on the surface of aluminum anode increases the overpotential of parasitic hydrogen evolution [31] and inhibits the cathodic process due to the competition of two cathodic reactions between the reduction of tin and water [7,32]. However, as the stannate concentration increases, tin gradually gathers on the surface of aluminum anode. It may give rise to dendritic growth, and consequently, shorten the lifetime of the cell [32,33]. Thus, 0.05 M Na_2SnO_3 is chosen as the appropriate solution and used in the following experiments.

As shown in Table 2, the hydrogen evolution rate of aluminum alloy in 4 M NaOH is further suppressed by the addition of casein. The 4 M NaOH electrolyte solution containing 0.05 M Na_2SnO_3 and $0.6\,g\,L^{-1}$ casein provides the optimal inhibition efficiency, with nearly one order of magnitude decrease in the corrosion rate compared with that in 4 M NaOH solution. However, the inhibition efficiency decreases if the concentration of casein exceeds $0.6\,g\,L^{-1}$. It is speculated that excess casein destroy the geometric coverage effect of hybrid inhibitor.

3.2. Electrochemical measurements

3.2.1. Open circuit potential measurements

The OCP of aluminum anode in 4 M NaOH containing different additives is displayed in Fig. 2. The OCP in the blank solution exhibits positive shift at initial period, due to the anode passivation resulting from the formation of insoluble oxide or hydroxide of aluminum [31,34]. Then the OCP reaches a steady state with the increase of the immersion time. While in solution with additives, the potential is much more positive at the beginning. The initial positive potential shift may be explained by the fact that casein molecules cover the aluminum surface and aggravate the anode polarization of aluminum. However, it changes to the negative potential direction latterly. The OCP shifts negatively to −1.801 V vs. Hg/HgO in the electrolyte solution with 0.05 M Na_2SnO_3 and $0.6\,g\,L^{-1}$ casein.

3.2.2. Polarization behaviors

Fig. 3 shows the potentiodynamic polarization curves of aluminum anode in 4 M NaOH with different inhibitors. The addition of inhibitors to the alkaline solution exhibits obviously more negative corrosion potentials as compared with the one in the blank solution. Especially, the presence of 0.05 M Na_2SnO_3 and
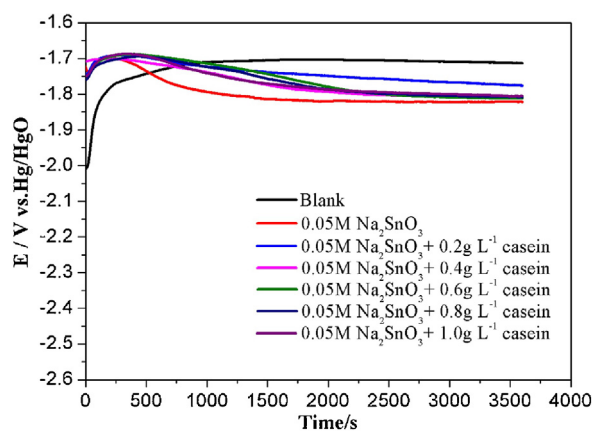

Fig. 2. OCP curves of aluminum anodes in 4 M NaOH solution containing different additives: no additive, 0.05 M Na_2SnO_3, 0.05 M Na_2SnO_3 with different contents of casein.

Table 2
Hydrogen evolution rates of Al alloy in 4 M NaOH with different inhibitors.

Solution(4 M NaOH +)	$R/m\,Lcm^{-2}\,min^{-1}$	IE/%
Blank solution	0.213	0
0.01 M Na_2SnO_3	0.143	32.86
0.03 M Na_2SnO_3	0.081	61.97
0.05 M Na_2SnO_3	0.064	69.95
0.07 M Na_2SnO_3	0.052	75.59
0.09 M Na_2SnO_3	0.068	68.07
0.05 M Na_2SnO_3 + 0.2 gL^{-1} casein	0.059	72.30
0.05 M Na_2SnO_3 + 0.4 gL^{-1} casein	0.048	77.46
0.05 M Na_2SnO_3 + 0.6 gL^{-1} casein	0.036	83.10
0.05 M Na_2SnO_3 + 0.8 gL^{-1} casein	0.047	77.93
0.05 M Na_2SnO_3 + 1.0 gL^{-1} casein	0.053	75.12

Fig. 3. Potentiodynamic curves of aluminum anodes in 4 M NaOH solution containing different additives: no additive, 0.05 M Na_2SnO_3, 0.05 M Na_2SnO_3 with different contents of casein.
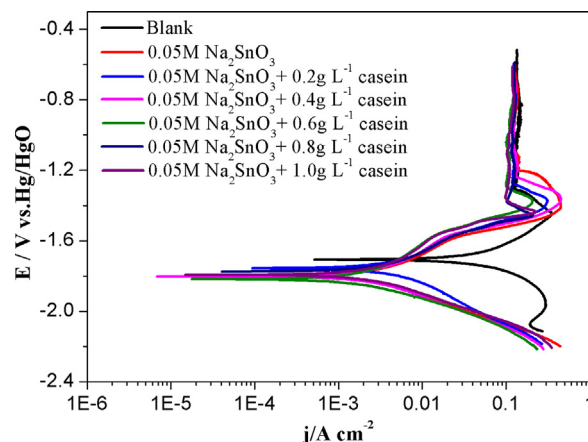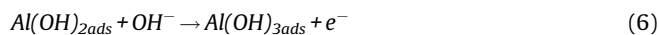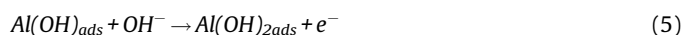
$0.6\,g\,L^{-1}$ casein in the alkaline solution results in a much more negative shift of the corrosion potential to $-1.818\,V$ vs. Hg/HgO. The cathodic current density of aluminum in additive-containing solution is clearly lower than that in blank one. It can be explained by the fact that the deposition of tin on the surface of aluminum anode improves the hydrogen overpotential and decreases the corrosion rate. Since the cathodic polarization curves in solution with additives are almost in parallel, the presence of casein should not alter the inhibition mechanism of Na_2SnO_3. Moreover, it is suspected that there is no chemical change taking place in casein.

In a wide potential window, aluminum exhibits a good anodic dissolution performance in different solution. The appearance of broad current peaks in the anodic curves may be attributed to the oxide reactions of alloy elements in aluminum. It is obvious that all the polarization curves in the anodic process have a limiting current, which is controlled by a multistep electrochemical process (4)–(7) [5]:

$$Al + OH^- \rightarrow Al(OH)_{ads} + e^- \qquad (4)$$

$$Al(OH)_{ads} + OH^- \rightarrow Al(OH)_{2ads} + e^- \qquad (5)$$

$$Al(OH)_{2ads} + OH^- \rightarrow Al(OH)_{3ads} + e^- \qquad (6)$$

$$Al(OH)_{3ads} + OH^- \rightarrow Al(OH)_{4ads} \qquad (7)$$

The diffusion of $Al(OH)_{1-4ads}$ ions has an important influence on the anode dissolution and under the limiting current condition, the electrochemical system proceeds at the maximum rate [26,35]. The electrochemical polarization for aluminum anode in different solution shows the similar limiting current. This phenomenon makes it clear that the addition of inhibitors does not have an impact on the dissolution of aluminum.

Considering the strong decrease in the cathodic process of aluminum anode, one can deduce that Na_2SnO_3 and casein hybrid inhibitor in alkaline solution promotes the inhibition effect. And the optimal effect appears when the concentration of casein is $0.6\,g\,L^{-1}$ in hybrid inhibitor.

3.2.3. Electrochemical impedance spectroscopy studies

Fig. 4 shows Nyquist plots for aluminum anode in different electrolyte solutions. The results in Fig. 4(b) exhibit that all the Nyquist plots contain a semi-circle with the real axis intercept at high frequency and a line at low frequency. It verifies that the addition of inhibitors didn't influence the reaction mechanism of anodes, but change the detailed parameters that have influence on the reaction process, which is consistent with the conclusion drawn from the potentiodynamic polarization curves.

The corresponding equivalent circuits of Nyquist plots are given in Fig. 4(a). Rs represents the solution resistance and increase a little bit with the addition of inhibitors, which suggests that additives didn't have obvious effect on solution resistance. The high frequency capacitive loop is caused by the charge-transfer resistance $(Rct_{,1})$ and double-layer capacitance (CPE_1). The electrolyte solutions with additives show higher $Rct_{,1}$ compared

Fig. 5. XRD spectra obtained from the surface of aluminum anodes after 1 h exposure in 4 M NaOH solution containing different additives. [(○) aluminum phase, (◇) tin phase, (△,☆) inherent material phases which almost do not participate in any reaction referred.
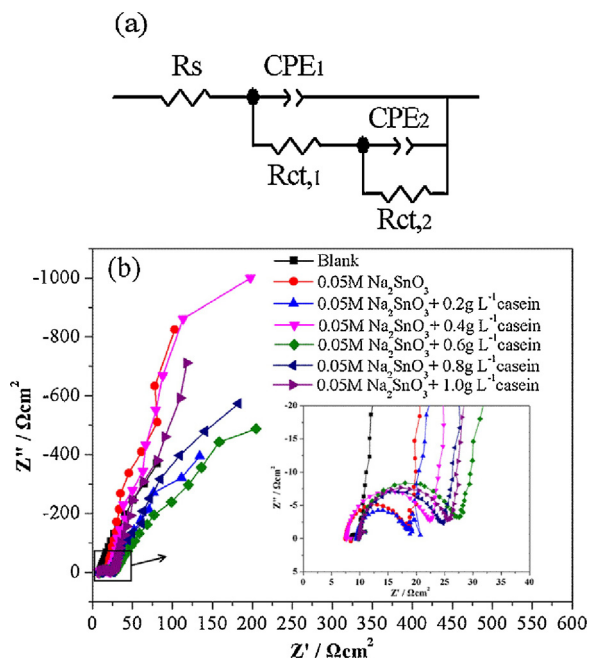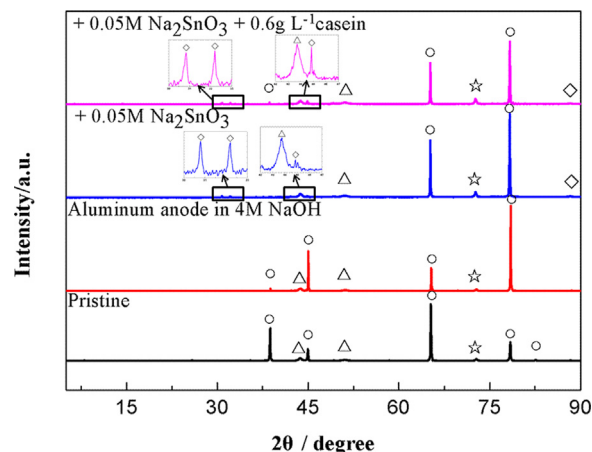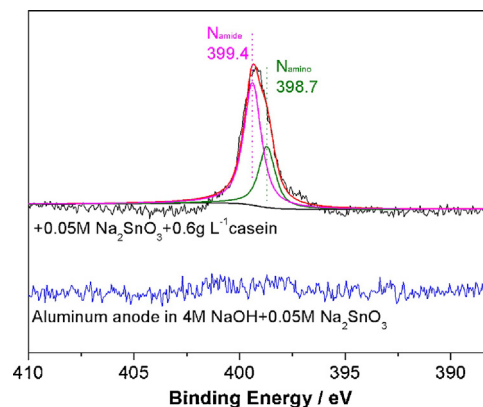
Fig. 4. The equivalent circuit of electrochemical impedance spectra (a), Nyquist plots of aluminum anodes in 4 M NaOH solution containing different additives (b).

Fig. 6. N1 s XPS spectra of aluminum anodes after 1 h exposure under OCP in 4 M NaOH solution containing different additives: 0.05 M Na_2SnO_3, 0.05 M Na_2SnO_3 and $0.6\,g\,L^{-1}$ casein.
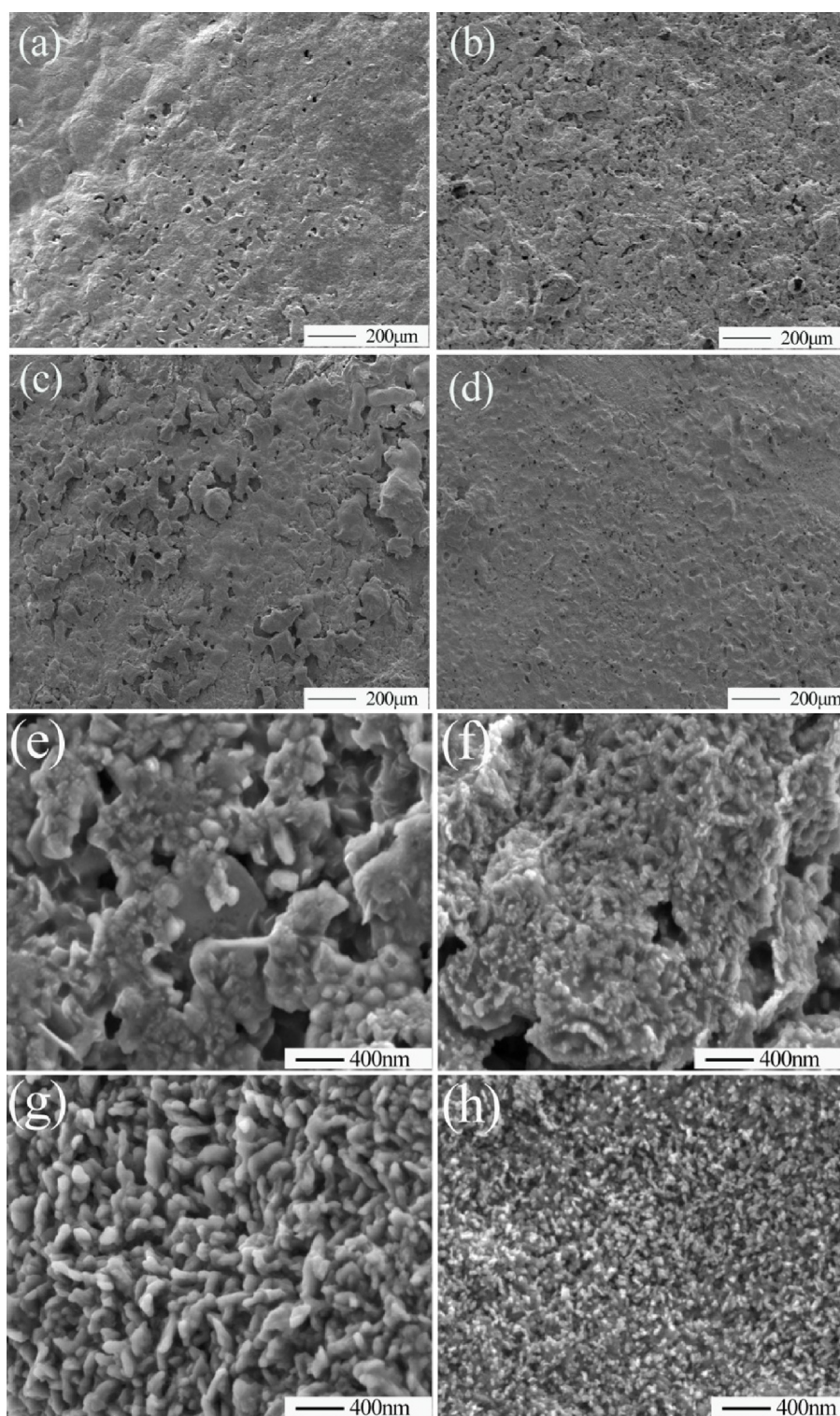
Fig. 7. SEM micrographs at low (×100) and high (×30000) resolution of aluminum anode surface after 1 h exposure under OCP in 4 M NaOH solution containing different additives: (a, e) blank, (b, f) 0.05 M Na_2SnO_3, (c, g) 0.6 g L^{-1} casein, (d, h) 0.05 M Na_2SnO_3 and 0.6 g L^{-1} casein.

with blank NaOH solution. Especially, the maximum charge transfer resistance exists in the anode with 0.05 M Na_2SnO_3 and 0.6 g L^{-1} casein, which indicates that the most stable protective layer composed of casein molecules and deposited tin is formed. This result is in highly coincidence with the hydrogen evolution test. The plots at low frequency might be a part of another capacitive loop, which is caused by the dissolution precipitation on the alloy surface [30]. In conclusion, the gathering of casein molecules and deposited tin on the aluminum surface brings surface geometry coverage. With the hybrid inhibitor system of

0.05 M Na_2SnO_3 and 0.6 g L^{-1} casein, the corrosion rate of aluminum anode reduces to as tiny as 0.036 ml cm^{-2} min^{-1}.

3.3. Surface composition analysis

As the aluminum electrode is immersed in the alkaline solution containing Na_2SnO_3, a deposited tin layer is supposed to cover its surface by the following reaction:

$$SnO_3{}^{2-} + 3H_2O + 4e^- \rightarrow Sn + 6OH^- \tag{8}$$
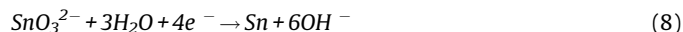
The crystalline structures of the aluminum anode were studied after exposing to different alkaline solution for one hour. The XRD spectra are displayed in Fig. 5. The recorded peaks are mainly identified as aluminum and tin phases (the enlarged figures), corresponding to PDF numbers 04-0787 and 04-0673, respectively. Obviously, the peak intensity of aluminum alloy in different solution changes prominently. This can be explained by the transforming of crystal plane orientation and crystal structure during the dissolution process of aluminum alloy. The appearance of metallic tin peaks can only be seen in the XRD spectra obtained from the solution with inhibitors, which can be ascribed to the weak adsorption ability of deposited tin on the surface of aluminum. It is determined that tin deposited on the aluminum surface decreases the active area and increases the hydrogen overpotential, and subsequently, suppresses the hydrogen evolution rate. However, the tin content shows no obvious variation in solution with hybrid inhibitors compared with the one with Na_2SnO_3, which can be roughly deduced from the peak intensity of tin.

Fig. 6 shows the N 1 s spectra of aluminum anodes after 1 h exposure under OCP in alkaline solution with different additives. The N 1 s spectrum of aluminum anode exposed in solution with 0.05 M Na_2SnO_3 and 0.6 g L^{-1} casein was fitted with two contributions, which are related to amino and amide groups in casein. N_{amino} atoms have more negative charge than N_{amide} atoms. Therefore, the peak at the lower binding energy of 398.7 eV is attributed to N_{amino} 1s, and the second peak with a binding energy of 399.4 eV is assigned to N_{amide} 1 s [36]. The peak area ratio of (N_{amide} 1s): (N_{amino} 1s) is about 2: 1, and it indicates that casein contains more amide groups. Therefore, it is proved that casein molecule is adsorbed on the surface of aluminum anode.

3.4. Surface micro-morphology analysis

The morphology of aluminum anode after 1 h exposure under OCP in alkaline solution with different inhibitors are shown in Fig. 7.

It is observed that the surface morphology of aluminum obviously depends on the composition of solution. Strong roughness, rigidity and high porosity can be clearly found on the anode surface in the blank solution in Fig. 7(a). Fig. 7(b) exhibits a loose lamellar on the surface of aluminum in 4M NaOH solution with Na_2SnO_3, which performs a tendency to peel. The layer in Fig. 7(c) is uneven and more likely to form the congeries, leading to the shedding of casein and heterogeneous dissolution of aluminum. A coralliform surface layer can be observed from Fig. 7(g), the high-resolution imagine in solution with single casein. Therefore, a web-like surface adsorption structure of casein can be inferred. While the presence of Na_2SnO_3 and casein hybrid inhibitor facilitates the formation of a pronounced uniformity and finer porous layer which can be further observed from the high-resolution SEM imagine of Fig. 7(h).

It can be concluded that the presence of casein promotes the deposition of tin on the alloy surface to be homogenized and stable. Besides, the addition of casein enhances the surface geometric coverage effect and restrains the aggregation and shedding of tin. The above results give reasonable explanation to the excellent corrosion inhibition and dissolution of anode in hybrid inhibitor system.

The schematic diagram of the possible hybrid inhibition mechanism is shown in Fig. 8. The deposited tin layer on the surface of aluminum is uneven and apt to pulling off in the solution with Na_2SnO_3. While in the solution with hybrid inhibitors, the polar functional groups in casein molecules are easy to be adsorbed on the aluminum surface, and conducive to the uniform deposition and adsorption of metallic tin. Compared with other organic inhibitors, such as polyaniline, polypyrrole, hydroxytryptamine and dimethyl amine epoxypropane, casein contains carbonyl group, amide group and amino group. Literature suggests that carbonyl group shows stronger absorption ability on the surface of aluminum [26]. In contrast with amino acids, casein has much more polar functional groups, which provides a better geometric coverage on the surface of aluminum. Thus, the complex layer becomes more stable and provides stronger corrosion protection.

3.5. Cell performance

The aluminum-air fuel cells were tested in galvanostatic method to evaluate the performance of aluminum anode in different electrolyte solutions. The conductivity of electrolyte solution with different additives is given in Table 3, and it is concluded that the addition of Na_2SnO_3 and casein didn't have significant effect on the conductivity of electrolyte. Before the galvanostatic test, the aluminum electrodes were exposed in different solutions at OCP for 1 h to form protective layers on aluminum anode surfaces.

As can be seen from Fig. 9, the cell performance with additives is obviously improved. As Na_2SnO_3 is added into the 4 M NaOH solution, the discharge capacity and cell voltage are much higher than the one without additives. However, the precipitation of tin in insoluble oxides will interfere with electrolyte management [37],
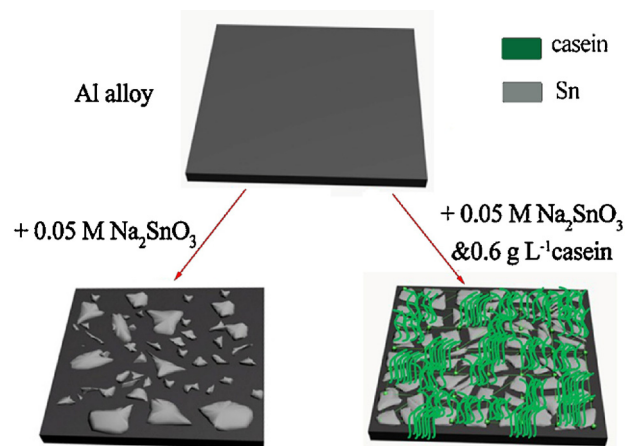

Fig. 8. The schematic illustrations of the hybrid inhibition mechanism.

Table 3
The conductivity of 4 M NaOH solution with different inhibitors.

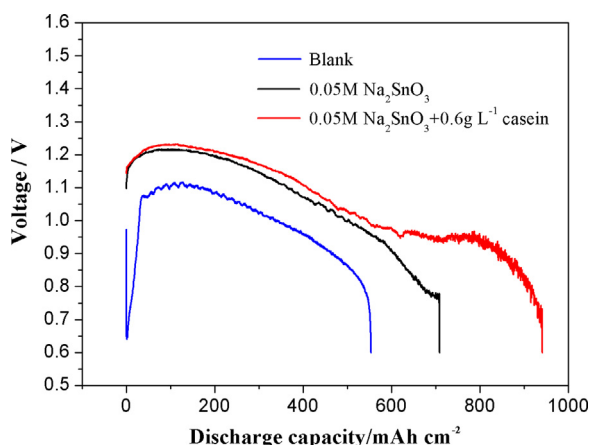| Solution(4 M NaOH +)	conductivity/mS cm^{-1}
Blank solution	394.1
0.05 M Na_2SnO_3	385.2
0.05 M Na_2SnO_3 + 0.6 gL^{-1} casein	384.1

Fig. 9. Cell performance of aluminum-air fuel cells at current density of $100\,mA\,cm^{-2}$ in 4 M NaOH solution containing different additives: no additive, $0.05\,M\,Na_2SnO_3$, $0.05\,M\,Na_2SnO_3$ and $0.6\,g\,L^{-1}$ casein.

and make aluminum-air fuel cell have the risk of short circuit. While aluminum-air fuel cell with $0.05\,M\,Na_2SnO_3$ and $0.6\,g\,L^{-1}$ casein hybrid inhibitor system exhibits the highest discharge capacity (9411 mAh) and discharge voltage compared with two other ones. The discharge capacity, especially, is approximately twice as much as the one with no additives. These results can further demonstrate that the relatively strong adsorption of casein facilitates the uniform deposition of tin, avoids the formation of dendrite, and promotes the dissolution of aluminum surface.

4. Conclusions

In this work, a new Na_2SnO_3 and casein hybrid inhibitor is proposed to alleviate the corrosion of aluminum anode in alkaline solution. The corrosion inhibition is achieved mainly by suppressing the cathodic reaction process of aluminum anode. The hydrogen evolution rate is decreased by around one order of magnitude in the electrolyte of 4 M NaOH containing $0.05\,M$ Na_2SnO_3 and $0.6\,g\,L^{-1}$ casein. In addition, the aluminum anode presents a much negative corrosion potential of $-1.818\,V$ vs. Hg/HgO with the hybrid inhibitor. Moreover, the discharge capacity at a high current density is almost twice as much as that in blank electrolyte solution. The hydrogen evolution inhibition mechanism is also proposed. That is, the strong adsorption of casein based on the coordination bond between aluminum ions and casein molecules promotes the uniform deposition of tin and enhances the surface geometric coverage of aluminum. Due to the remarkable performance of corrosion inhibition and excellent cell performance, this new hybrid organic-inorganic inhibitor system is promising to drive the practical application of aluminum-air fuel cells, especially for a high power output.

Acknowledgements

References

[1] M.A. Rahman, X. Wang, C. Wen, High Energy Density Metal-Air Batteries: A Review, Journal of The Electrochemical Society 160 (2013) A1759–A1771.

[2] D. Wang, H. Li, J. Liu, D. Zhang, L. Gao, L. Tong, Evaluation of AA5052 alloy anode in alkaline electrolyte with organic rare-earth complex additives for aluminium-air batteries, Journal of Power Sources 293 (2015) 484–491.

[3] Z. Sun, H. Lu, Q. Hong, L. Fan, C. Chen, J. Leng, Evaluation of an Alkaline Electrolyte System for Al-Air Battery, ECS Electrochemistry Letters 4 (2015) A133–A136.

[4] M. Pino, J. Chacón, E. Fatás, P. Ocón, Performance of commercial aluminium alloys as anodes in gelled electrolyte aluminium-air batteries, Journal of Power Sources 299 (2015) 195–201.

[5] D.R. Egan, R.J.K. Ponce de León, R.L. Jones, K.R. Stokes, F.C. Walsh, Developments in electrode materials and electrolytes for aluminium–air batteries, Journal of Power Sources 236 (2013) 293–310.

[6] M. Pino, C. Cuadrado, J. Chacon, P. Rodriguez, E. Fatas, P. Ocon, The electrochemical characteristics of commercial aluminium alloy electrodes for Al/air batteries, Journal of Applied Electrochemistry 44 (2014) 1371–1380.

[7] M. Mokhtar, M.Z.M. Talib, E.H. Majlan, S.M. Tasirin, Recent developments in materials for aluminum–air batteries: A review, Electrochimica Acta 4 (2015) 1–20.

[8] J. Ma, J. Wen, J. Gao, Q. Li, Performance of Al-0.5 Mg-0.02 Ga-0.1 Sn-0.5 Mn as Anode for Al-Air Battery, Journal of the Electrochemical Society 161 (2014) A376–A380.

[9] J. Ma, J. Wen, H. Zhu, Q. Li, Electrochemical performances of Al-0.5Mg-0.1Sn-0.02In alloy in different solutions for Al-air battery, Journal of Power Sources 293 (2015) 592–598.

[10] D.D. Macdonald, S. Real, M. Urquidi-Macdonald, Evaluation of Alloy Anodes for Aluminum-Air Batteries: III. Mechanisms of Activation, Passivation, and Hydrogen Evolution, Journal of The Electrochemical Society 135 (1988) 2397–2409.

[11] J. Ma, J. Wen, J. Gao, Q. Li, Performance of Al–0. 5 Mg–0. 02 Ga–0. 1 Sn–0. 5 Mn as anode for Al–air battery in NaCl solutions, Journal of Power Sources 253 (2014) 419–423.

[12] D. Mercier, M.G. Barthés-Labrousse, The role of chelating agents on the corrosion mechanisms of aluminium in alkaline aqueous solutions, Corrosion Science 51 (2009) 339–348.

[13] A.M.M.M. Adam, N. Borràs, E. Pérez, P.L. Cabot, Electrochemical corrosion of an Al-Mg-Cr-Mn alloy containing Fe and Si in inhibited alkaline solutions, Journal of Power Sources 58 (1996) 197–203.

[14] M. Paramasivam, M. Jayachandran, S. Venkatakrishna Iyer, Influence of alloying additives on the performance of commercial grade aluminium as galvanic anode in alkaline zincate solution for use in primary alkaline batteries, Journal of Applied Electrochemistry 33 (2003) 303–309.

[15] S.Z. El Abedin, A.O. Saleh, Characterization of some aluminium alloys for application as anodes in alkaline batteries, Journal of Applied Electrochemistry 34 (2004) 331–335.

[16] L. Bockstie, D. Trevethan, S. Zaromb, Control of Al Corrosion in Caustic Solutions, Journal of The Electrochemical Society 110 (1963) 267–271.

[17] X. Chang, J. Wang, H. Shao, J. Wang, X. Zeng, J. Zhang, C. Cao, Corrosion and Anodic Behaviors of Pure Aluminum in a Novel Alkaline Electrolyte, Acta Physico-Chimica Sinica 24 (2008) 1620–1624.

[18] D. Gelman, I. Lasman, S. Elfimchev, Y.E.-E.D. Starosvetsky, Aluminum Corrosion Mitigation in Alkaline Electrolytes By Hybrid Inorganic/Organic Inhibitor System for Power Sources Applications, Journal of Power Sources 285 (2015) 100–108.

[19] Z. Sun, H. Lu, Performance of Al-0.5In as Anode for Al-Air Battery in Inhibited Alkaline Solutions, Journal of the Electrochemical Society 162 (2015) A1617–A1623.

[20] A. Elango, V. Periasamy, M. Paramasivam, Study on polyaniline-ZnO used as corrosion inhibitors of 57S aluminium in 2 M NaOH solution, Anti-Corrosion Methods and Materials 56 (2009) 266–270.

[21] I.L. Lehr, S.B. Saidman, Characterisation and corrosion protection properties of polypyrrole electropolymerised onto aluminium in the presence of molybdate and nitrate, Electrochimica Acta 51 (2006) 3249–3255.

[22] I.L. Lehr, S.B. Saidman, Electrodeposition of polypyrrole on aluminium in the presence of sodium bis(2-ethylhexyl) sulfosuccinate, Materials Chemistry and Physics 100 (2006) 262–267.

[23] J.B. Wang, J.M. Wang, H.B. Shao, X.T. Chang, L. Wang, J.Q. Zhang, C.N. Cao, The corrosion and electrochemical behavior of pure aluminum in additive-containing alkaline methanol–water mixed solutions, Materials and Corrosion 60 (2009) 269–273.

[24] X.Y. Wang, J.M. Wang, H.B. Shao, J.Q. Zhang, C.N. Cao, Influences of zinc oxide and an organic additive on the electrochemical behavior of pure aluminum in an alkaline solution, Journal of Applied Electrochemistry 35 (2005) 213–216.

[25] D. Gelman, I. Lasman, S. Elfimchev, D. Starosvetsky, Y. Ein-Eli, Aluminum corrosion mitigation in alkaline electrolytes containing hybrid inorganic/organic inhibitor system for power sources applications, Journal of Power Sources 285 (2015) 100–108.

[26] D. Wang, L. Gao, D. Zhang, D. Yang, H. Wang, T. Lin, Experimental and theoretical investigation on corrosion inhibition of AA5052 aluminium alloy by l-cysteine in alkaline solution, Materials Chemistry and Physics 169 (2016) 142–151.

[27] P.S.D. Brito, C.A.C. Sequeira, Organic Inhibitors of the Anode Self-Corrosion in Aluminum-Air Batteries, Journal of Fuel Cell Science and Technology 11 (2013) 011008–011008.

[28] D. Wang, D. Zhang, K. Lee, L. Gao, Performance of AA5052 alloy anode in alkaline ethylene glycol electrolyte with dicarboxylic acids additives for aluminium-air batteries, Journal of Power Sources 297 (2015) 464–471.

[29] J. Ma, J. Wen, J. Gao, Q. Li, Performance of Al-1Mg-1Zn-0.1Ga-0.1Sn as anode for Al-air battery, Electrochimica Acta 129 (2014) 69–75.

[30] L. Fan, H. Lu, J. Leng, Z. Sun, Performance of Al-0.6 Mg-0.05 Ga-0.1 Sn- 0.1 In as Anode for Al-Air Battery in KOH Electrolytes, Journal of The Electrochemical Society 162 (2015) A2623–A2627.

[31] M.L. Doche, J.J. Rameau, R. Durand, F. Novel-Cattin, Electrochemical behaviour of aluminium in concentrated NaOH solutions, Corrosion Science 41 (1999) 805–826.

[32] D.S. Stoychev, E.A. Stoyanova, S. Rashkov, Deposition of thin tin coatings on aluminium alloys, Surface Technology 23 (1984) 127–141.

[33] P.W. Jeffrey, W. Halliop, F.N. Smith, Aluminum anode alloy, (1988) United States.

[34] D.D. Macdonald, S. Real, S.I. Smedley, M. Urquidi-Macdonald, Evaluation of Alloy Anodes for Aluminum-Air Batteries: IV. Electrochemical Impedance Analysis of Pure Aluminum in at 25 °C, Journal of The Electrochemical Society 135 (1988) 2410–2414.

[35] C. Ponce-de-León, C.T.J. Low, G. Kear, F.C. Walsh, Strategies for the determination of the convective-diffusion limiting current from steady state linear sweep voltammetry, Journal of Applied Electrochemistry 37 (2007) 1261–1270.

[36] B.B. Hurisso, K.R.J. Lovelock, P. Licence, Amino acid-based ionic liquids: using XPS to probe the electronic environment via binding energies, Physical Chemistry Chemical Physics 13 (2011) 17737–17748.

[37] G.M. Scamans, W.B. O'Callaghan, N.P. Fitzpatrick, R.P. Hamlen, Present status of aluminum-air battery development, 21st Intersociety Energy Conversion Conference, American Chemical Society, San Diego, 1986, pp. 1057–1061.